

A Truncated Form of Nef Selected during Pathogenic Reversion of Simian Immunodeficiency Virus SIVmac239 Δ nef Increases Viral Replication

Lisa A. Chakrabarti,^{1*} Karin J. Metzner,² Tijana Ivanovic,³ Hua Cheng,³ Jean Louis-Virelizier,¹ Ruth I. Connor,³ and Cecilia Cheng-Mayer³

*Viral Immunology Unit, Pasteur Institute, Paris, France*¹; *Institute of Clinical and Molecular Virology, University of Erlangen-Nuremberg, Erlangen-Nuremberg, Germany*²; and *Aaron Diamond AIDS Research Center, The Rockefeller University, New York, New York*³

Received 11 July 2002/Accepted 30 September 2002

The live, attenuated vaccine simian immunodeficiency virus SIVmac239 Δ nef efficiently protects rhesus macaques against infection with wild-type SIVmac but occasionally causes CD4⁺ T-cell depletion and progression to simian AIDS (SAIDS). Virus recovered from a vaccinated macaque (Rh1490) that progressed to SAIDS had acquired an additional deletion in the *nef* gene, resulting in a frameshift that restored the original *nef* open reading frame (R. I. Connor, D. C. Montefiori, J. M. Binley, J. P. Moore, S. Bonhoeffer, A. Gettie, E. A. Fenamore, K. E. Sheridan, D. D. Ho, P. J. Dailey, and P. A. Marx, *J. Virol.* 72:7501-7509, 1998). Intravenous inoculation of the Rh1490 viral isolate into four naive rhesus macaques induced CD4⁺ T-cell depletion and disease in three out of four animals within 2 years, indicating a restoration of virulence. A DNA fragment encompassing the truncated *nef* gene amplified from the Rh1490 isolate was inserted into the genetic backbone of SIVmac239. The resulting clone, SIVmac239- Δ 2nef, expressed a Nef protein of approximately 23 kDa, while the original SIVmac239 Δ nef clone expressed a shorter protein of 8 kDa. The revertant form of Nef did not cause downregulation of CD4, CD3, or major histocompatibility complex class I. The infectivity of SIVmac239- Δ 2nef was similar to that of SIVmac239 Δ nef in single-cycle assays using indicator cell lines. In contrast, SIVmac239- Δ 2nef replicated more efficiently than SIVmac239 Δ nef in peripheral blood mononuclear cell (PBMC) cultures infected under unstimulated conditions. The p27 Gag antigen levels in SIVmac239- Δ 2nef-infected cultures were still lower than those obtained with wild-type SIVmac239, consistent with a partial recovery of Nef function. The transcriptional activity of long terminal repeat (LTR)-luciferase constructs containing the *nef* deletions did not differ markedly from that of wild-type LTR. Introduction of a premature stop codon within Nef- Δ 2 abolished the replicative advantage in PBMCs, demonstrating that the Nef- Δ 2 protein, rather than the structure of the U3 region of the LTR, was responsible for the increase in viral replication. Taken together, these results show that SIV with a deletion in the *nef* gene can revert to virulence and that expression of a form of *nef* with multiple deletions may contribute to this process by increasing viral replication.

The *nef* gene is essential for achieving the full pathogenic potential of primate lentiviruses. In a seminal study, Kestler et al. showed that deletion of the *nef* gene markedly reduced the capacity of simian immunodeficiency virus (SIV) to induce AIDS in rhesus macaques (19). Animals infected with SIV carrying a 182-bp deletion in *nef* were chronically infected but retained a low viral load for several years without signs of CD4⁺-T-cell depletion or progression to disease. Very similar characteristics have been reported in rare cases of human infections with human immunodeficiency virus type 1 (HIV-1) strains having *nef* deletions. Large *nef* deletions were initially documented in one hemophiliac patient infected since 1983 (21) and in an Australian cohort of six long-term nonprogressors (LTNP) who had been infected by blood from a single donor (10). More subtle mutations, such as small deletions and point mutations that inactivate only some functions of Nef,

have also been reported in LTNP (5, 20). The notion that *nef* mutations can lead to virus attenuation is supported by the finding that forms with *nef* deletions can be detected in up to 10% of infections with HIV-2, a lentivirus associated with a longer clinical latency than HIV-1 (38).

Lentiviruses with *nef* deletions were proposed as candidates for the development of live attenuated vaccines against HIV. In the rhesus macaque model, SIVmac with a *nef* deletion (SIVmac239 Δ nef) did confer protection against superinfection with wild-type SIVmac239 and other closely related strains of SIV (9, 42). Protection was dependent on the duration of SIVmac Δ nef infection and typically developed at around 10 to 15 weeks postvaccination (7, 18). SIVmac carrying deletions in multiple accessory genes, including *nef*, also conferred protection, although vaccine efficacy correlated inversely with the degree of viral attenuation (18). Live, attenuated SIV and HIV represent the most effective vaccine candidates developed to date, but the potential use of these viruses in humans has raised serious concerns about their safety. Forms of SIVmac with multiple deletions, such as SIVmac239 Δ 3, cause simian AIDS (SAIDS) in newborn macaques and occasionally in adult

* Corresponding author. Mailing address: Unité d'Immunologie Virale, Institut Pasteur, 28 rue du Dr. Roux, 75724 Paris Cédex 15, France. Phone: 33-1-40 61 31 99. Fax: 33-1-45 68 89 41. E-mail: chakra@pasteur.fr.

animals (2). SIVmac239 carrying a 152-bp deletion in *nef* is frequently pathogenic in juvenile and newborn animals (34). SIVmac239 Δ *nef*, which has a 182-bp deletion in *nef*, can also induce AIDS in adult animals. We have previously observed a rapid progression to disease in 1 out of 16 adult rhesus macaques that were vaccinated with SIVmac239 Δ *nef* (7). In addition, long-term follow up revealed a consistent decrease in CD4⁺ T cells in other vaccinated macaques (R.I. Connor, unpublished observations). Recent findings with humans confirm that deletions in *nef* do not entirely eliminate HIV or SIV pathogenicity. Signs of disease progression, including loss of CD4⁺ T cells, increase in viral load, and, in one case, occurrence of opportunistic infection, have been observed in the Australian cohort of HIV- Δ *nef*-infected patients after 14 to 18 years of follow-up (23). Also, the hemophilic patient who has been infected since 1983 now has depleted CD4⁺ T cells, even though the viral load remains undetectable (14).

An unresolved issue is the mechanism by which viruses with *nef* deletions can become pathogenic. Long-term low-level replication may be enough to progressively impair the host immune system. Alternatively, viral evolution in the host may lead to the emergence of variants with increased pathogenicity. One striking instance of evolution in SIV carrying *nef* deletions is the progressive accumulation of additional deletions within the region of *nef* that overlaps with the upstream U3 sequences in the long terminal repeat (LTR) (22). Additional *nef* deletions also occur in humans, illustrating the parallel between HIV and SIVmac infections and the relevance of the simian model for *nef* analyses (10, 21). Mutagenesis studies of SIVmac239 suggest that the role of the *nef*-U3 overlapping sequences is primarily to code for the C-terminal region of Nef rather than to contribute to LTR function (15). Therefore, the accumulation of secondary *nef* deletions can be viewed as the result of selection pressures to remove nonfunctional sequences. However, additional deletions in *nef* can also result in gain-of-function mutations, when frameshifting puts the C-terminal part of the gene back in phase with the N-terminal part. Sawai et al. have shown that the synthesis of such truncated forms of Nef can be repeatedly selected for and can persist over time, raising the possibility that they contribute to virulence (34).

The present study focuses on a case of rapid reversion of SIVmac239 Δ *nef* to virulence. We demonstrate that the revertant virus has become pathogenic and has acquired the capacity to encode a Nef protein of intermediate length. Analysis of Nef properties shows that in spite of the absence of conserved core sequences, the truncated protein has retained the key capacity to increase viral replication in primary T cells.

MATERIALS AND METHODS

Animals and viruses. Four adult rhesus macaques (*Macaca mulatta*) were used in this study. The animals were seronegative for SIV and type D retroviruses before the initiation of the experiments. All protocols used in this study were reviewed and approved by an institutional animal care and use committee. The 1490 virus stock was obtained by cocultivation of peripheral blood mononuclear cells (PBMC) obtained from animal Rh1490 on day 167 postinfection with phytohemagglutinin (PHA)-stimulated PBMC from an uninfected rhesus macaque. The titer of the viral stock was determined on CEMx174 cells as previously described (7). The four naive rhesus macaques were infected by intravenous inoculation of 10⁴ 50% tissue culture infective doses of the 1490 viral stock on day 0. Blood samples collected in EDTA anticoagulant were used to deter-

mine SIV RNA levels in plasma, using a branched DNA (bDNA) signal amplification assay (Bayer Corporation) (8). The lower quantification limit of this assay was 1,500 viral RNA copies/ml or plasma until April 1999, when the assay was modified by the manufacturer to a limit of sensitivity of 400 copies/ml. Additional viral load measurements were done by real-time PCR and reached a sensitivity limit of 50 copies/ml (28).

Nef sequences. DNA was extracted from frozen PBMC obtained on either day 154 (macaque L259) or day 343 (macaques J344, J482, and L257) postinoculation by using a genomic DNA extraction kit (Qiagen). For comparison, DNA was also extracted from the original PBMC culture that was used to amplify the SIVmac1490 viral stock. A fragment encompassing the SIVmac *nef* gene was amplified by nested PCR with a mixture of *Taq* polymerase and the proofreading *Pwo* polymerase (Expand High Fidelity PCR system; Boehringer-Mannheim/Roche). PCRs were performed with the following primers: outer pair, TM1-Eco (5'-GGG AAT TCA AGA ATT GTT GCG ACT GAC CG-3') and USR1 (5'-AAA GCA GAA AGG GTC CTA ACA GAC CAG GG-3'); inner pair, preNhe (5'-CTG TTA AGA ATA GTG ATC TAT ATA GT-3') and USR2 (5'-GAC CAG GCG GCG ACT AGG AGA GAT GGG A-3').

PCR products were cloned in the pGEM-T Easy vector (Promega) and sequenced in both orientations. Sequence reactions performed with fluorescent deoxy- and dideoxynucleotides were analyzed with an automated 373A sequencer (PE Applied Biosystems).

Plasmids. All SIVmac proviral constructs were based on pBR239E, which contains the full SIVmac239 genome (GenBank accession number M33262) inserted in a pBR322-based vector. This plasmid, which has an *nef* open reading frame and contains a unique *EcoRI* site added at the end of the 3' LTR, was a generous gift from Toshiaki Kodama (Oregon Regional Primate Research Center). The proviral clone that contains the two *nef* deletions, pSIVmac239- Δ 2*nef*, was constructed by inserting the *SacI*-to-*BspMI* fragment (nucleotide [nt] 9486 to 10283 in sequence M33262) from clone 1490-27-7-1 into pBR239E. Proviral clone pSIVmac239-N contains three silent mutations in the N terminus of Nef, which cause amino acid changes in the Env. This plasmid was engineered by inserting the *NheI*-to-*SacI* fragment (nt 8998 to 9486) of clone 1490-27-7-1 into the pBR239E backbone. Proviral clone pSIVmac239-N Δ 2*nef*, which contains both the Env transmembrane glycoprotein changes and the two *nef* deletions, was obtained by insertion of the 1490-27-7-1 *NheI*-to-*BspMI* fragment (nt 8998 to 10283) into pBR239E. The proviral clone that contains the original *nef* deletion, pSIVmac239 Δ *nef*, was derived from plasmid p239SpE3'- Δ Nef, which was initially described by Kestler et al. and contains the 3' half of the SIVmac239 genome with a 182-bp *nef* deletion (19). High-fidelity PCR was used to amplify p239SpE3'- Δ Nef sequences from the *NheI* site (nt 8998) to the 3' end of the genome and to add an *EcoRI* site at the 3' end. The *NheI*-to-*EcoRI* fragment was fully sequenced and inserted in pBR239E to generate pSIVmac239 Δ *nef*. All pBR322-based plasmids containing SIVmac proviral genomes were propagated in JM109 bacteria grown at 30°C to limit the potential for recombination between the two LTR copies.

Introduction of a stop codon after the amino acid at position 20 of *nef* was done by PCR with overlapping mutagenic oligonucleotides. A 5' *nef* fragment (nt 9156 to 9405) was amplified with primers FcccXba (5'-TCG ATC TAG AAT ATA TTC ATT TCC TGA TCC GCC-3') and Nefstop2R (5'-CCA CGC GCC CGC TAG AGT CTC TGT CG-3'). The 3' *nef* fragment (nt 9381 to 9736) was obtained with primers Nefstop2 (5'-CGA CAG AGA CTC TAG CGG GCG CGT GG-3') and CpriR (5'-CTG TAA TAA ATC CCT TCC AGT CCC-3') (mutated nucleotides are underlined). The two fragments were gel purified, joined by reamplification with FcccXba and CpriR, cloned in pGEM-Teasy vector (Promega), and sequenced. The resulting fragment was reinserted into clone pBR239E (containing the 239 wild-type genome) to yield p239-WTstop and into clone p239- Δ 2*nef* (containing the Δ 2 deletion) to yield p239- Δ 2*nef* stop.

Inserts for bicistronic Nef expression vectors were generated by amplification of *nef* sequences with primers FcccXba and RLTRcBam (3'-TCG AGG ATC CCA GGG CTC AAT CTG CCA GCC TC-3') by high-fidelity PCR. Inserts were sequenced, digested with *XbaI* and *BamHI*, and cloned into the *NheI* and *BamHI* sites of the pIRES2-EGFP vector (Clontech). The resulting constructs contained the *nef* and enhanced green fluorescent protein (EGFP) genes separated by an internal ribosome entry site, which permitted both genes to be translated from a single bicistronic mRNA.

To generate Nef-GFP fusion proteins, *nef* sequences were inserted into the pEGFP-N3 vector (Clontech) so that the *nef* open reading frame was in phase with that of EGFP. Nef sequences (plus 177 bp of 5' flanking sequences) were amplified with primers FcccXba and R-3'*nef*-Bam (5'-GAT GGA TCC GCG AGT TTC CTT CTT GTC AGC-3'), sequenced, digested with *XbaI* and *BamHI*, and inserted into the polylinker of pEGFP-N3.

To generate LTR-luciferase reporter plasmids, a *SacI*-to-*HincII* fragment (nt

9486 to 10450) encompassing a 3' fragment of the *env* gene, the whole of U3 and R, and 35 bp of U5 was cloned into the polylinker of pGL3-Basic (Promega). The resulting constructs expressed the luciferase gene under the control of the SIV LTR.

Infections. Viral stocks were generated by transfection of 3 μ g of genomic SIVmac plasmids in 293T cells plated at 4×10^5 cells/well in six-well plates. Transfection was performed with the DMRIE-C reagent according to the recommendations of the manufacturer (Gibco-BRL). Cell culture supernatants were harvested at 72 h posttransfection, centrifuged at $800 \times g$, filtered through 0.45- μ m-pore-size filters, and stored at -70°C until use. The amount of SIV was quantified by using a p27 Gag enzyme-linked immunosorbent assay kit (Beckman Coulter). Normalized viral stocks containing 50 ng of p27 Gag antigen were used to infect 10^7 unstimulated human or macaque PBMC for 3 h at 37°C . The cells were then washed and cultivated at 3×10^6 cells/ml in RPMI 1640 medium supplemented with 10% fetal calf serum, penicillin, and streptomycin (RPMI-c). Cultures were stimulated 2 days postinfection by addition of PHA at $1 \mu\text{g}/10^6$ cells and interleukin-2 (IL-2) at 10 U/ml. Viral production was monitored by measurement of SIV p27 Gag in culture supernatants.

Single-cycle infectivity assays (or Magi assays) were done with HeLa-derived cell lines that expressed CD4 and a relevant coreceptor and that were transduced with the β -galactosidase gene under the control of the HIV-1 LTR. P4-R5 cells expressing human CCR5 (provided by Pierre Charneau, Institut Pasteur) were propagated in Dulbecco's modified Eagle medium plus 10% fetal calf serum, penicillin, and streptomycin (DMEM-c) supplemented with $1 \mu\text{g}$ of puromycin per ml. Magi-RhR5 cells expressing rhesus macaque CCR5 (provided by Zhiwei Chen, Aaron Diamond AIDS Research Center [ADARC]) were propagated in DMEM-c with 200 μg of G418 per ml and $1 \mu\text{g}$ of puromycin per ml. The cells were plated at a density of 4×10^4 cells/well in 24-well plates and infected the next day with viral supernatants containing 20 or 50 ng of SIV p27 Gag antigen in the presence of 10 μg of DEAE-dextran per ml. On day 3 postinfection, the cells were fixed in 1% paraformaldehyde and 0.2% glutaraldehyde, washed, and incubated in staining solution containing $1 \times$ phosphate-buffered saline (PBS), 4 mM potassium ferrocyanide, 4 mM potassium ferricyanide, 2 mM MgCl_2 , and 400 μg of X-Gal (5-bromo-4-chloro-3-indolyl- β -D-galactopyranoside) per ml. Cell were stained for 50 min to 2 h at 37°C in a non- CO_2 incubator and washed twice in PBS. The number of blue cells per well was counted under an optical microscope.

Immunoblot. CEMx174 cells were resuspended in 100 μ l of protein extraction buffer containing 50 mM Tris (pH 8.0), 137 mM NaCl, 2 mM EDTA, 10% glycerol, 1% Nonidet P-40 detergent, and the protease inhibitors aprotinin, leupeptin, and Pefablock at 1 $\mu\text{g}/\text{ml}$ each. The protein extracts were incubated for 10 min on ice and clarified in an Eppendorf microcentrifuge for 10 min at 14,000 rpm. Extracts were resuspended in $2 \times$ sodium dodecyl sulfate loading buffer for analysis by immunoblotting as previously described (26). To detect deletion forms of the Nef proteins, samples were run on a 12% polyacrylamide gel and immunoblotted with a polyclonal rabbit anti-SIVmac Nef serum generously provided by Paul Luciw (University of California, Davis) (34). Nef-GFP fusion protein expression in transfected HEK 293T cells was detected with an anti-GFP antibody (Santa Cruz Biotechnology) used at a 1:10,000 dilution.

Fluorescence imaging. 293T cells were seeded onto round coverslips coated with poly-L-lysine and were grown in DMEM-c. The cell were transfected the next day with Nef-GFP fusion vectors by using the DMRIE-C reagent (Gibco-BRL). Transfected cells were fixed after 48 h in PBS with 1% paraformaldehyde. Cells attached to the coverslips were mounted in Vectashield medium with DAPI (4',6'-diamidino-2-phenylindole) (Vector laboratories). Images were obtained and deconvolved through a DeltaVision restoration microscopy system utilizing Softworx software (Applied Precision).

Analysis of LTR transcriptional activity. LTR-luciferase plasmid constructs were electroporated into Jurkat-E6 cells (provided by Rong Liu, ADARC). Twenty micrograms of plasmid DNA resuspended in 50 μ l of 0.15 M NaCl was used per electroporation. Each DNA sample consisted of 10 μg of the pLTR-luc construct to be tested, 5 μg of the HIV-1 Tat expression vector pTat13, and 5 μg of the constitutive β -galactosidase expression vector pBC12/CMV/lacZ (27). Cells were grown in RPMI-c and maintained at concentrations lower than 3×10^5 cells/ml prior to each experiment. 10^7 cells were resuspended in 200 μ l of RPMI-c and added to 50 μ l of DNA mix in 0.4-cm electroporation cuvettes. Electroporation was carried out at 250 V and 960 μF by using a Gene Pulser II apparatus with capacitance extender (Bio-Rad). Luciferase and β -galactosidase activities were tested 24 to 48 h later with the Luciferase Assay System (Promega) and the Galacto-Star (Tropix) kits.

Flow cytometry. The downregulation of cell surface markers was evaluated by flow cytometry in cells expressing Nef constructs. Three types of Nef-expressing cells were generated. HeLa-CD4 cells were transfected with bicistronic Nef/

EGFP expression vectors. Jurkat E6 cells, which express CD3, were electroporated with bicistronic Nef/EGFP plasmids as described above. To evaluate major histocompatibility complex class I (MHC-I) downregulation, the reporter cell line CEMx174 5.25 (a kind gift from Nathaniel Landau, Salk Institute) was infected with SIVmac clones. This cell line is stably transduced with CCR5 and with an HIV-1-LTR-GFP reporter construct, so that infected cells are positive for GFP expression. Antibodies used for surface staining included anti-CD4-allophycocyanin (Exalpha, Boston, Mass.), anti-CD3-phycoerythrin (clone SP34; PharMingen BDIS), and anti-HLA class I-phycoerythrin (clone MHBC04; Caltag). Cells were resuspended in 100 μ l of PBA buffer (PBS plus 1% bovine serum albumin and 10 mM NaN₃), incubated for 15 min at room temperature in the presence of labeled antibodies, washed in PBA buffer, and resuspended in PBA buffer with 1% paraformaldehyde. Analyses were performed by using a FACSCalibur flow cytometer with Cellquest software (Becton Dickinson). All analyses were performed on the GFP-positive population, which corresponded to Nef-expressing cells. Negative controls for GFP labeling consisted of cells transfected with the empty plasmid vector pCG or uninfected cells. The negative control for Nef expression consisted of cells transfected with the vector pIRES2-EGFP. The specificity of surface marker staining was assessed with isotype-matched control antibodies.

Nucleotide sequence accession numbers. The nucleotide sequences of the *nef* gene for the seven clones represented in Fig. 2 have been deposited in GenBank and are available under accession numbers AY129655 to AY129661.

RESULTS

The 1490 isolate is pathogenic. Previously, we reported on a case of disease progression in a rhesus macaque inoculated with live, attenuated SIVmac239 Δ nef (7). Infection in macaque Rh1490 was characterized by a peak viremia of 5×10^6 viral RNA copies/ml, a high viral load during the chronic stage of infection (up to 10^6 copies/ml), and a subsequent loss of CD4⁺ T cells. This animal was challenged with SIVmac251 at 10 weeks after SIVmac239 Δ nef inoculation, but the challenge virus remained undetectable by repeated nested-PCR testing of blood and lymph node samples, suggesting that pathogenic progression was due to replication of SIVmac239 Δ nef. At 2 years postinoculation, macaque Rh1490 had severely depleted CD4⁺ T cells (100 cells/mm³), developed SAIDS, and was euthanized. Viral sequences amplified from plasma and PBMC revealed an evolution of the *nef* gene, with the acquisition of additional *nef* deletions that became predominant at 12 weeks after infection and persisted at later time points (7).

The isolate obtained from animal Rh1490 at day 167 was propagated in macaque PBMC to generate a viral stock (SIVmac1490). The virus was then passaged into four naive adult rhesus macaques by intravenous inoculation of 10^4 50% tissue culture infective doses of SIVmac1490. Peak viremia in the four macaques ranged between 10^6 and 10^7 viral RNA copies/ml (Fig. 1A). Comparison with historical controls showed that macaques infected with SIVmac1490 had significantly higher viremia peaks than macaques infected with the original SIVmac239 Δ nef clone, with mean viral RNA copy numbers of 4×10^6 versus $1 \times 10^6/\text{ml}$ (Fig. 1C) (7). However, SIVmac1490 still induced lower viremia peaks than the highly pathogenic SIVmac251 isolate (mean RNA copy number for SIVmac251, $7 \times 10^7/\text{ml}$). Three of the four macaques inoculated with the 1490 isolate showed signs of CD4 depletion and disease progression (Fig. 1B). Animal L259 progressed rapidly to disease and was euthanized on day 193 because of wasting associated with chronic diarrhea. This animal had a transient rebound of viremia that preceded a drop of CD4⁺-T-cell numbers, and it died with depleted CD4⁺ T cells ($145/\text{mm}^3$) and signs of colitis. Animal J482 maintained a chronically high viral load and developed SAIDS at 1.5 years after inoculation. At necropsy,

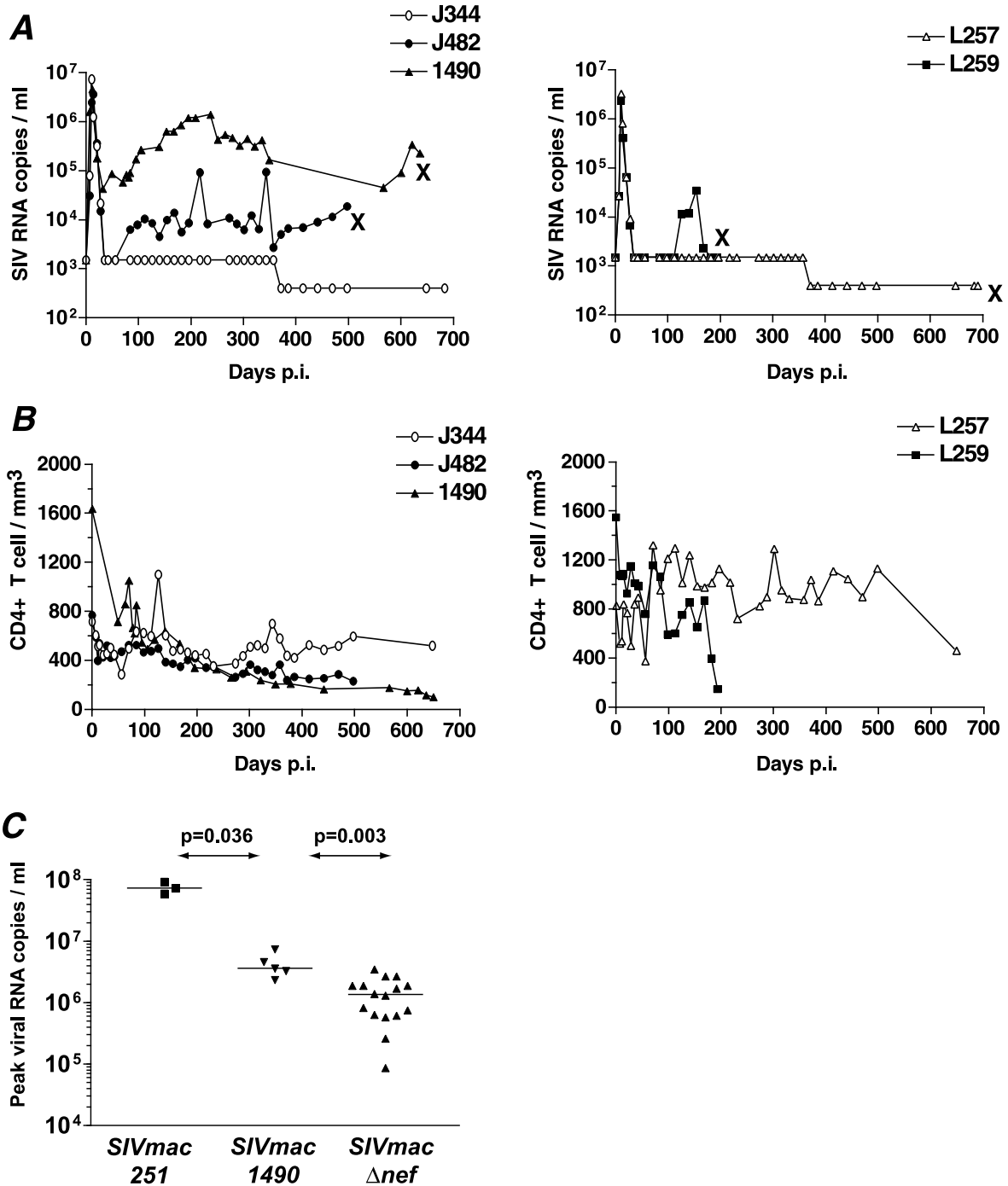


FIG. 1. Viral load and CD4⁺-T-cell counts in macaques infected with SIVmac with *nef* deleted. (A and B) Number of viral RNA copies per milliliter of plasma (A) and number of CD4⁺ T cells per cubic millimeter of blood (B) for the SIVmac239Δ*nef*-infected animal (1490) that spontaneously progressed to disease and the four rhesus macaques (J344, J482, L257, and L259) inoculated with the SIVmac1490 isolate. ×, time of death. The viral load was measured by the bDNA assay (8), which had a lower detection limit of 1,500 copies/ml until day 370 and of 400 copies/ml afterwards. p.i., postinfection. (C) Comparison of peak viral RNA values induced by different SIVs during primary infection. Data for animals infected with the pathogenic isolate SIVmac251 and the attenuated molecular clone SIVmac239Δ*nef* were obtained from a previous study (7). Comparisons between groups were made with the nonparametric Mann-Whitney test (*P* values are indicated above arrows; median values are indicated by horizontal bars).

J482 had a low CD4⁺ T-cell count (230/mm³), a viral load of 2 × 10⁴ copies/ml, and evidence of opportunistic infection with *Pneumocystis carinii*. Macaque L257 developed signs of disease and was euthanized 2 years postinoculation, with moderate

CD4⁺ T-cell depletion (464/mm³) and undetectable viremia as measured by bDNA assays (<400 RNA copies/ml). Additional testing by real-time PCR, using primers and a molecular beacon that surround the original *nef* deletion (28), also yielded

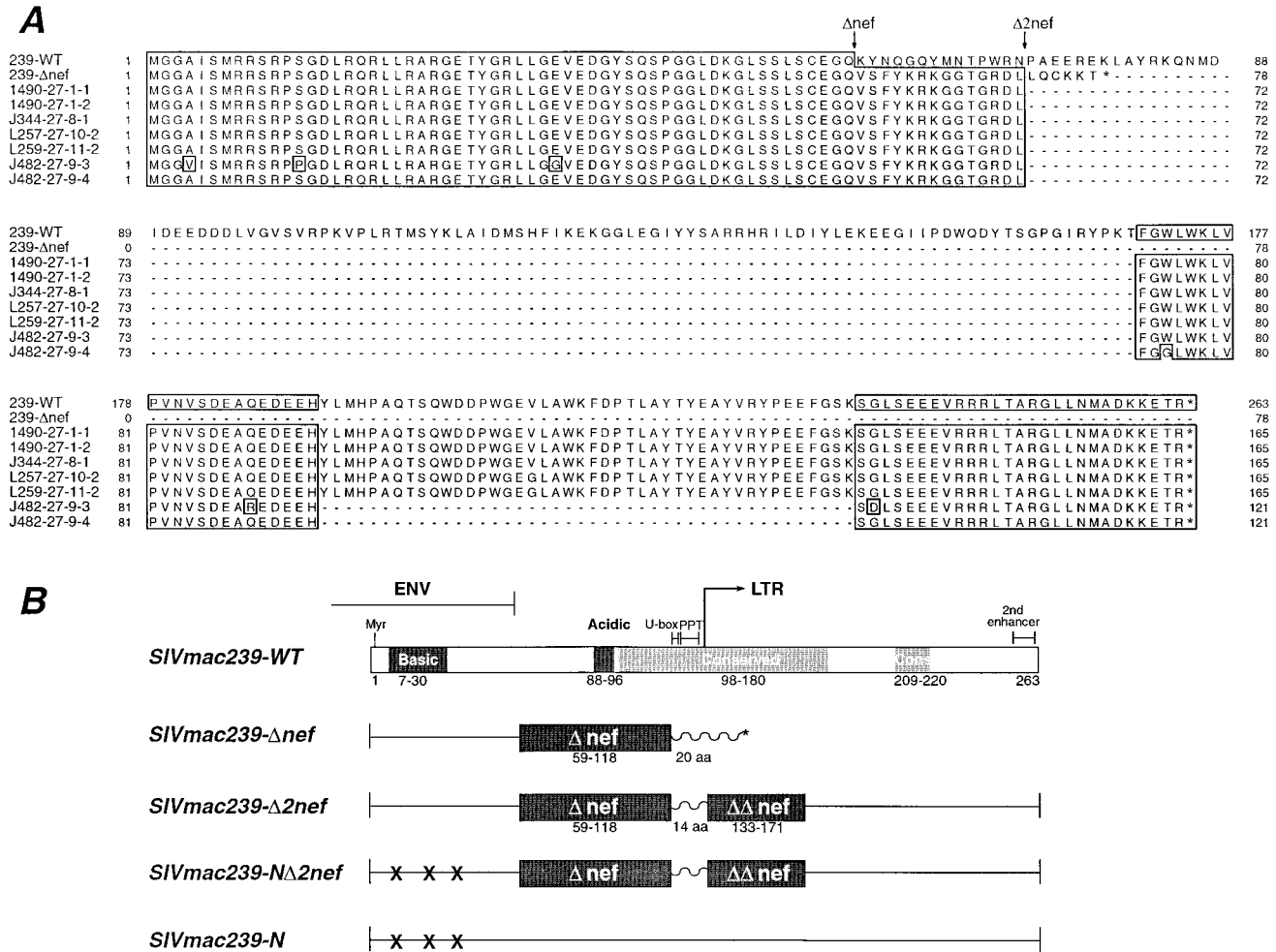


FIG. 2. Alignment and schematic representation of Nef sequences. (A) Alignment of Nef protein sequences from the original molecular clone (239- Δ nef), the SIVmac1490 viral isolate (clones 1490-27-1-1 and -27-1-2), and the viruses amplified from the four rhesus macaques inoculated with the SIVmac1490 isolate (clones J344-27-8-1 to J482-27-9-4). Regions of the alignment with amino acid identity of greater than 70% are boxed. The positions of the original deletion (Δ nef) and of the additional deletion characteristic of the 1490 virus (Δ 2nef) are indicated by arrows. (B) Schematic diagrams of SIVmac wild type and with *nef* deletions. Features of Nef such as the myristylation site (Myr), the basic and acidic regions, and the two conserved regions (shaded in gray) are indicated. The overlapping *env* open reading frame (ENV) and important *cis*-acting regions, such as the U box, the polypurine tract (PPT), the 3' end of the LTR (arrow), and the recently described second enhancer (17) are also indicated. The structure of Nef for SIVmac molecular clones used in the study is shown below that of the wild-type protein. Deletions are represented by solid boxes. Wavy lines correspond to amino acid sequences that are frameshifted compared to wild-type Nef, and the asterisk indicates a termination codon. The X signs correspond to silent mutations in *nef* that change the amino acid sequence in the overlapping *env* gene.

undetectable viremia, with a threshold of detection of 50 copies/ml. Necropsy findings included colitis complicated by amyloid deposits in the small intestine and lymphoid hyperplasia. The fourth macaque, J344, had moderately depleted CD4⁺ T cells (466/mm³ at day 683) and remained healthy throughout a 2-year observation period. These findings showed that the SIVmac1490 isolate was more pathogenic than SIVmac239 Δ nef, since three out of four inoculated macaques progressed to disease within 2 years of infection. Pathogenesis induced by SIVmac1490 virus nevertheless differed from that induced by wild-type SIVmac in that clinical progression could occur in the presence of a moderate to low plasma viral load.

The nef- Δ 2 deletion is maintained upon in vivo passage. We characterized the *nef* deletions present in the 1490 virus isolate and its evolution upon in vivo passage. DNA was extracted from the macaque PBMC used to propagate the 1490 virus

stock and from the PBMC of the four inoculated macaques. A 1.2-kb fragment encompassing the *nef* open reading frame was amplified by high-fidelity PCR, cloned, and sequenced (Fig. 2A). Genetic analysis revealed that the 1490 virus had acquired a 112-bp deletion in addition to the original 182-bp deletion present in the SIVmac239 Δ nef clone. Interestingly, the second deletion, termed Δ 2, reversed the frameshift introduced by the original deletion and led to a longer *nef* open reading frame (Fig. 2B). The predicted Nef- Δ 2 protein was 165 amino acids (aa) in length and lacked the acidic domain and most of the conserved core region of wild-type Nef (Nef-WT). However, it retained the flexible N-terminal domain and the long C-terminal domain specific to SIVmac. Importantly, the Δ 2 deletion preserved the *cis*-acting sequences needed for viral replication, including the U box, the polypurine tract, the *att* site needed for integration, and the viral enhancers (16, 33).

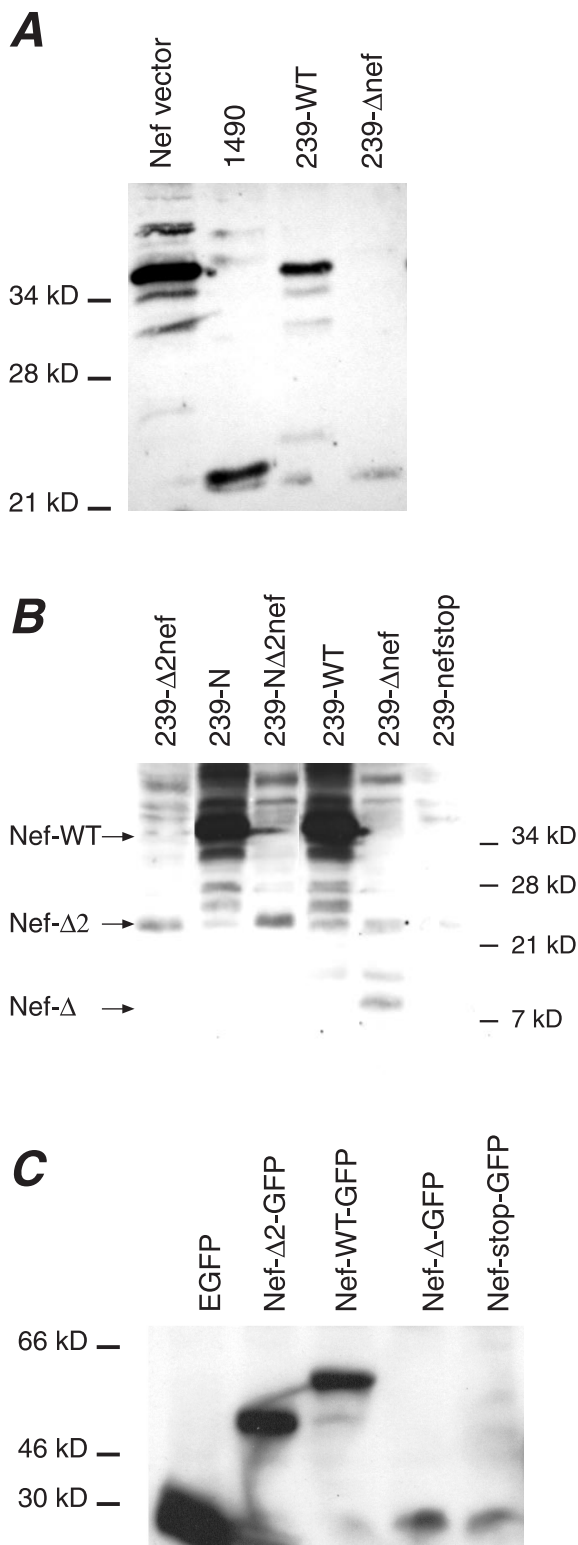


FIG. 3. Expression of truncated Nef proteins. Protein extracts from infected CEMx174 cells were immunoblotted with an anti-SIVmac Nef polyclonal serum. (A) A truncated Nef protein with an apparent molecular mass of 23 kDa was detected in cells infected with the 1490 isolate (second lane), while Nef-WT was detected at approximately 35 kDa in extracts from SIVmac239-infected cells (third lane) and in 293T cells transfected with an SIVmac Nef expression vector (first lane). These bands were absent in extracts from SIVmac239 Δ nef-infected

Nef sequences from the four inoculated macaques were analyzed at either 6 months (L259) or 1 year (L257, J344, and J482) postinoculation. Sequence alignment showed that the $\Delta 2$ deletion was conserved upon in vivo passage (Fig. 2A). The predicted amino acid sequence of *nef* was unchanged in three macaques (L257, L259, and J344), while in the fourth (J482), *nef* acquired a third deletion of 132 bp which resulted in a predicted protein of 122 aa lacking most of the C-terminal domain. Clones from J482 also contained nonconservative amino acid substitutions that suggested a possible loss of Nef function. For each animal, the PCR products obtained from PBMC DNA were homogeneous in size, suggesting that the deletions identified in sequenced clones were representative of the viral quasispecies in vivo (data not shown). Evaluation of nucleotide substitutions in *nef* indicated that the maximum divergence was of 0.65% for macaque J344 (not taking the deletion into account) and 0 to 0.25% for the other three animals. Thus, in most macaques, sequences coding for Nef- $\Delta 2$ showed little genetic evolution upon in vivo passage.

The truncated form of Nef is expressed and localizes to a vesicular compartment. We next assessed whether the truncated form of Nef could contribute to SIV replication and thus account for the pathogenic phenotype of SIVmac1490. We chose to focus on the Nef- $\Delta 2$ form that predominated in Rh1490 and in three out of four reinoculated macaques. Constructs were derived from a clone that represented the consensus sequence of the 1490 isolate. An *NheI*-to-*BspMI* fragment encompassing the *nef* gene of SIVmac1490 clone 27-1-1 was introduced in the SIVmac239 genetic backbone. The resulting clone, SIVmac239-N $\Delta 2$ nef, differed from SIVmac239 by the presence of the two deletions in addition to three point mutations in the N terminus of *nef* (C9063T, A9110G, and C9263T). These mutations were silent in *nef* but changed the amino acid sequence of the overlapping *env* open reading frame (T735I, R751G, and L802F). To rule out possible effects of *env* mutations, we also constructed clone SIVmac239- $\Delta 2$ nef, which contained the two *nef* deletions but not the three point mutations. An additional control consisted of the reciprocal construct SIVmac239-N, which contained the three point mutations in *env* but not the *nef* deletions (Fig. 2B).

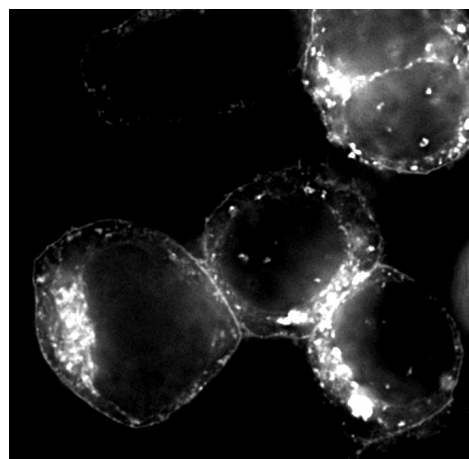
Nef expression was tested by immunoblotting with protein extracts from infected CEMx174 cells and a polyclonal anti-SIV Nef rabbit serum for detection. Cells infected with the SIVmac1490 isolate were found to express a truncated form of Nef that migrated with an apparent molecular mass of approximately 23 kDa (Fig. 3A). This was slightly higher than the

cells (fourth lane). (B) Detection of Nef in CEMx174 cells infected with different SIVmac molecular clones. A band corresponding to Nef- $\Delta 2$ is seen in cells infected with SIVmac239- $\Delta 2$ nef and SIVmac239-N- $\Delta 2$ nef (first and third lanes, respectively). A nonspecific band migrates just below the position of Nef- $\Delta 2$ and is visible in the SIVmac239 Δ nef-infected cells (fifth lane). A small protein of approximately 9 kDa corresponds to the expected molecular mass of the Nef- Δ protein encoded by SIVmac239 Δ nef. (C) Expression of Nef-GFP fusion proteins. HEK 293T cells transfected with Nef-GFP expression vectors were analyzed by immunoblotting with an anti-GFP monoclonal antibody. Nef- Δ -GFP and Nef-stop-GFP serve as negative controls, since the presence of in-frame stop codons in *nef* prevents the expression of the fusion proteins.

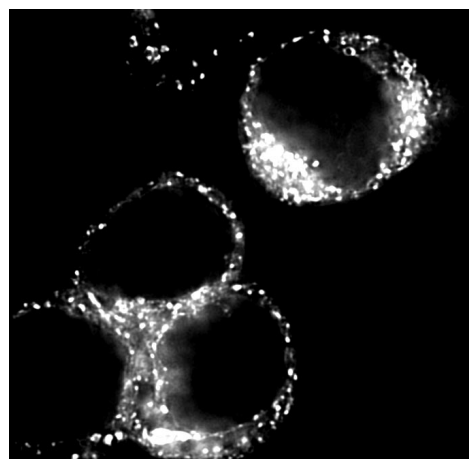
predicted molecular mass of 18.7 kDa for Nef- $\Delta 2$ and may be explained by posttranslational modifications such as myristylation or phosphorylation. No other *nef*-specific bands were detected, indicating that the SIVmac1490 isolate expressed a single truncated form of Nef. Molecular clones SIVmac239- $\Delta 2$ nef and SIVmac239-N $\Delta 2$ nef expressed a truncated Nef protein of the same size as that detected in SIVmac1490-infected cells (Fig. 3B). The lower expression levels detected for Nef- $\Delta 2$ compared to Nef-WT could be attributed in part to the absence of epitopes recognized by the polyclonal rabbit serum. Indeed, when expressed as GFP fusions in transfected HEK 293T cells, comparable amounts of Nef- $\Delta 2$ -GFP and Nef-WT-GFP proteins could be detected with an anti-GFP monoclonal antibody (Fig. 3C). An even smaller form of Nef could be detected in cells infected with SIVmac239 Δ nef but was absent from cells infected with SIVmac239-nef stop, which has a nonsense codon at position 93 in Nef (Fig. 3B). The Nef- Δ protein had an apparent molecular mass of 8 to 10 kDa, compatible with a predicted molecular mass of 8.5 kDa. Therefore, truncated Nef proteins consisting of the N-terminal domain only or the joint N- and C-terminal domains were expressed in the context of a productive SIVmac infection.

HEK 293T cells transfected with Nef-GFP expression vectors were examined by fluorescence deconvolution microscopy to assess whether the presence of the $\Delta 2$ deletion had any effect on Nef subcellular localization. Nef- $\Delta 2$ -GFP localized mainly to a vesicular compartment, similar to the wild-type protein Nef-WT-GFP (Fig. 4). Minor differences in the repartition of GFP-positive vesicles were observed, with Nef-WT-GFP localizing mainly to a perinuclear area, while Nef- $\Delta 2$ -GFP was more homogeneously distributed in cytoplasmic vesicles. The vesicular localization of Nef- $\Delta 2$ suggests that this protein retained the capacity to interact with the endocytic machinery.

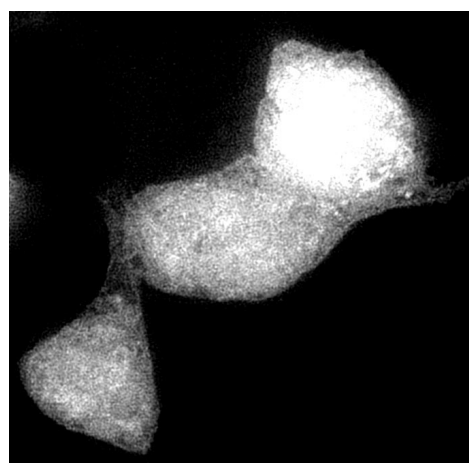
Nef $\Delta 2$ does not downregulate cell surface receptors. To assess the functional properties of Nef- $\Delta 2$, we engineered bicistronic expression vectors that coded for both Nef and EGFP proteins. Transfection of these vectors in HeLa-CD4 cells and analysis of the GFP-positive population by flow cytometry allowed the evaluation of CD4 expression in the subpopulation of cells that expressed Nef (Fig. 5A). As expected, Nef-WT caused a downregulation of CD4 cell surface expression. In contrast, Nef- $\Delta 2$ gave a CD4 expression profile indistinguishable from that of Nef- Δ (Fig. 5A) or a control GFP vector (not shown). Electroporation of Nef expression vectors in Jurkat-E6 cells showed that, in the context of a T lymphoid cell line, Nef-WT downregulated both the CD4 and CD3 receptors. Within the GFP-positive population, 80% of the CD3^{low} cells were also CD4^{low}, supporting the notion that Nef has a dual effect on CD4 and CD3. In contrast, expression of Nef- $\Delta 2$ did not modify the surface expression of either of these receptors (Fig. 5B). We next assessed the effect of Nef on MHC-I expression levels. Downregulation of MHC-I in Jurkat cells by the Nef-WT expression vector was low but detectable (not shown). To better evaluate the effect of Nef on MHC-I expression, additional experiments were performed in the context of a productive SIV infection. CEMx174 5.25 cells, which are transduced with CCR5 and an LTR-GFP cassette, were infected with different SIVmac molecular clones and analyzed by flow cytometry at 6 days postinfection. The numbers of infected cells, as evaluated by the percentage of GFP-positive



Nef-WT-GFP



Nef- $\Delta 2$ -GFP



Vector-GFP

FIG. 4. Localization of Nef-GFP fusion proteins. 293T cells transfected with Nef-GFP expression vectors were visualized by fluorescence deconvolution microscopy. Nef-WT and Nef- $\Delta 2$ localized to a vesicular compartment, while the unfused EGFP protein encoded by vector pEGFP-N3 had a homogenous cytoplasmic distribution. Magnification, $\times 100$.

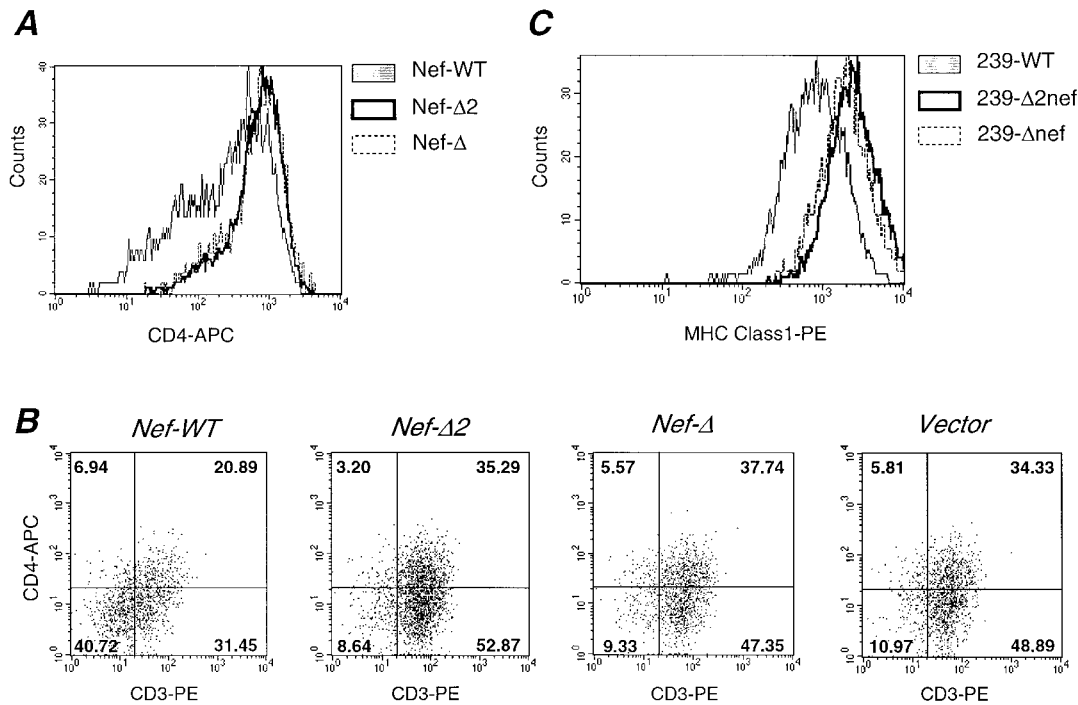


FIG. 5. Absence of cell surface marker downregulation by truncated Nef proteins. (A) HeLa-CD4 cells transfected with bicistronic Nef-EGFP vectors were analyzed by flow cytometry for CD4 downregulation. Analyses were done on the GFP-positive population of cells that expressed Nef. (B) Jurkat E6 cells electroporated with bicistronic Nef-EGFP vectors were analyzed for CD3 and CD4 downregulation. The percentage of cells in each quadrant is indicated. (C) CEMx174 5.25 cells were infected with recombinant SIVmac239 clones that expressed wild-type Nef (239-WT) or Nef with deletions (239- Δ 2nef and 239- Δ nef). The population of infected cells (GFP positive) was analyzed for MHC-I downregulation at day 6.

cells, were equivalent for the different molecular clones and ranged between 18 and 24%. Analysis of MHC-I expression within the GFP-positive population showed that only SIVmac239 expressing Nef-WT caused MHC-I downregulation (Fig. 5C). This set of experiments shows that the truncated Nef- Δ 2 protein has lost the capacity to downregulate the surface receptors CD4, CD3, and MHC-I.

Nef- Δ 2 increases SIVmac replication in unstimulated primary cells. A key property of HIV and SIV Nef proteins is the ability to increase viral replication in unstimulated primary T cells. To test whether this property was retained by Nef- Δ 2, unstimulated human PBMC were infected with virus produced from the different SIVmac molecular clones after first normalizing for p27 Gag antigen concentration. Cultures were stimulated at 2 days postinfection with PHA and IL-2, and were monitored for p27 Gag production for 3 weeks. This culture protocol has been successfully used to reveal the delayed replication kinetics of Nef mutants in PBMC cultures (29, 36). As shown in Fig. 6A, SIVmac239- Δ 2nef and SIVmac-239-N Δ 2nef showed replication levels that were intermediate between those of the wild-type virus and those of SIVmac239 Δ nef. A similar phenotype was observed in rhesus macaque PBMC cultures, where viruses carrying the Nef- Δ 2 deletion reached p27 levels close to those obtained with the wild-type virus 2 weeks after infection (Fig. 6B). Since SIV replication in PBMC culture is known to be variable and to depend on the donor, we repeated the infection experiments five times, using different human PBMC donors and two independent viral stocks. In each case, SIVmac239- Δ 2nef replicated to levels intermediate between those seen with wild-type SIVmac239 and SIVmac239 Δ nef. For

each experiment, p27 values were compared at the day of peak viral replication for the wild-type virus (Fig. 6C). This analysis confirmed that SIVmac239- Δ 2nef replicated to higher levels than SIVmac239 Δ nef and to lower levels than wild-type SIVmac239, with the differences being statistically significant ($P = 0.03$ in both cases). Therefore, the Nef- Δ 2 allele partially restored SIV replication capacity in primary T cells. No significant differences were observed between the replication of SIVmac239- Δ 2nef and SIVmac-239-N Δ 2nef (Fig. 6A and B), indicating that the three point mutations in *env* did not modify SIVmac replication in a primary T-cell culture system.

Infectivity of the different SIV molecular clones was next assessed in single-cycle Magi assays. Viral supernatants normalized for p27 Gag content were used to infect HeLa-CD4 cells transduced with an LTR- β -galactosidase reporter cassette and human CCR5 (P4-R5 cells) (Fig. 6D). The infectivity of viruses carrying the Δ 2 deletion was indistinguishable from that of SIVmac239 Δ nef or SIVmac239-nefstop and was reduced fivefold compared to that of clones expressing Nef-WT (Fig. 6D). Similar experiments were conducted with Magi-RhR5, a second indicator cell line that expresses rhesus macaque CCR5. This cell line proved to be more susceptible to SIV infection and gave a higher differential (15- to 20-fold) between the infectivities of wild-type and mutant clones. Even with this more sensitive assay, the infectivities of SIVmac-239 Δ 2nef and SIVmac-239-N Δ 2nef did not differ significantly from that of SIVmac239-nefstop (Fig. 6E). Taken together, these data showed that infectivity enhancement in fibroblastic cell lines and increased viral replication in primary T cells were properties that could be dissociated. The truncated Nef- Δ 2 protein facilitated SIV replication only in primary T

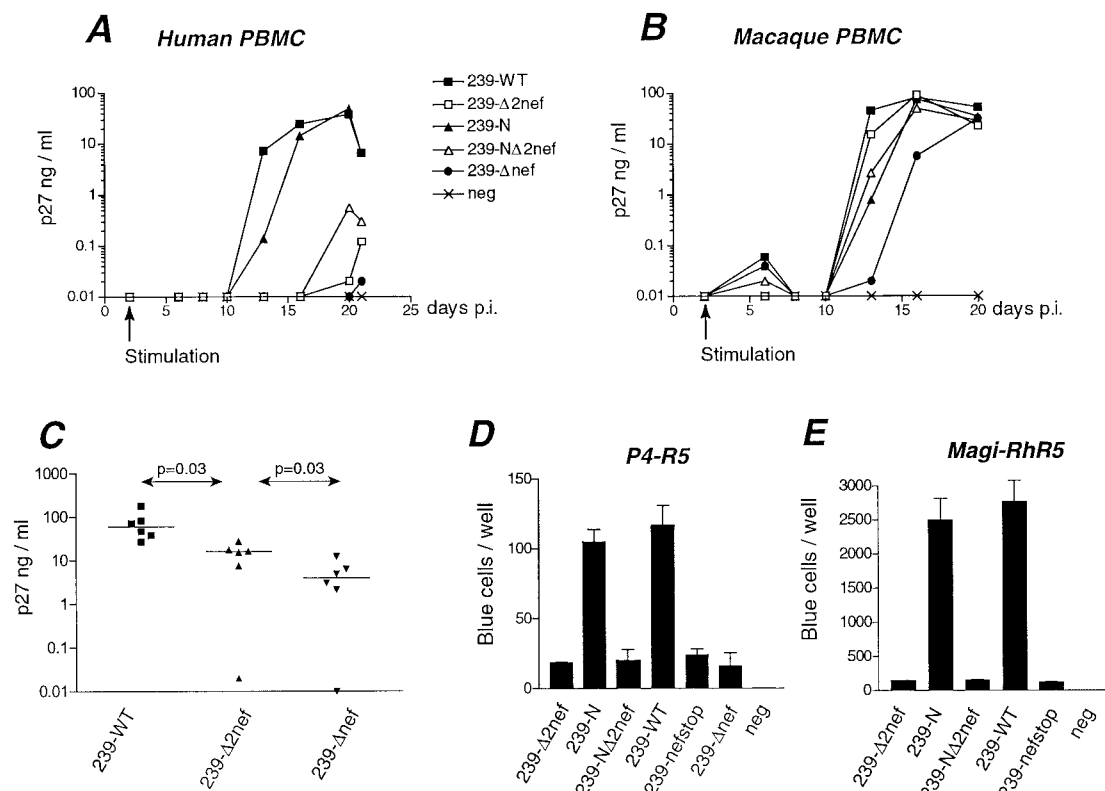


FIG. 6. Nef-Δ2 increases SIVmac replication in primary T cells. (A) Human PBMC were infected with different SIVmac molecular clones and were left unstimulated for 2 days before PHA and IL-2 were added to the cultures. Viral replication was monitored for 3 weeks by measuring the amount of SIV Gag p27 antigen in culture supernatants. p.i., postinfection. (B) Similar infections were done with rhesus macaque PBMC. (C) Comparison of infection experiments with PBMC from six different human donors. p27 values obtained at the day of peak viral replication for the wild-type virus are plotted. Comparisons between groups were made with the nonparametric Wilcoxon test for paired samples; *P* values are indicated above arrows, and median values are indicated by horizontal bars. (D) Single-cycle infectivity of SIVmac molecular clones was measured by infection of P4-R5 cells that express CD4, human CCR5, and β-galactosidase under the control of the HIV-1 LTR. Infectivity was measured by the mean number of blue cells per well. Standard deviations for triplicate wells are indicated. neg, negative. (E) Similar experiments were done with Magi-R5 cells that express rhesus macaque CCR5 in place of human CCR5.

cells, suggesting that this phenotype was dependent on T-cell-specific factors.

Increased viral replication depends on Nef expression. The Δ2 deletion modified the structure of the Nef protein but also that of the overlapping U3 region of the LTR. In particular, this deletion resulted in the loss of modulatory sequences located 5' to the enhancer. It was therefore possible that the increased replication of SIVmac239-Δ2nef in primary T cells was due to altered transcriptional activity of the LTR. To test this possibility, we engineered LTR-luciferase constructs in which a *SacI*-to-*HincII* fragment encompassing the U3 and R regions of the SIV LTR drove the expression of a luciferase reporter gene. Jurkat E6 cells were electroporated with LTR-luciferase constructs, a Tat expression vector, and a β-galactosidase expression vector that was used to control for transfection efficiency. The transcriptional activity, as measured by the ratio of luciferase activity to β-galactosidase activity, did not differ markedly between the different LTR constructs (Fig. 7). pLTR-Δ2 was approximately 25% more efficient than pLTR-WT at driving luciferase expression and had an activity comparable to that of pLTR-Δ. All of the reporter constructs had similar activities when transfected in HeLa cells (not shown).

Since the Δ2 deletion did not appear to markedly increase

LTR transcriptional activity, a direct effect of the truncated Nef protein on viral replication seemed more likely. To test whether Nef-Δ2 expression was indeed required for increased viral replication, we engineered an SIVmac molecular clone in which the Nef-Δ2 open reading frame was interrupted by a premature termination codon after the amino acid at position 20. Infection of unstimulated human PBMC with the resulting clone, SIVmac239-Δ2nefstop, resulted in replication levels that were clearly decreased compared to those of SIVmac239-Δ2nef and that were equivalent to those of SIVmac239Δnef (Fig. 8). As a control, we verified that introduction of a nonsense codon at the same position in wild-type SIVmac239 also resulted in limited viral replication. Taken together, these results demonstrate that expression of the truncated Nef-Δ2 protein facilitates SIV replication in primary T cells.

DISCUSSION

This study provides evidence that SIVmac encoding a truncated Nef protein lacking the central core region is pathogenic in rhesus macaques. The virus from Rh1490, which contains two large deletions in *nef*, was passaged into naive macaques and induced disease in three out of four animals within 2 years. This isolate proved to be more pathogenic than the original

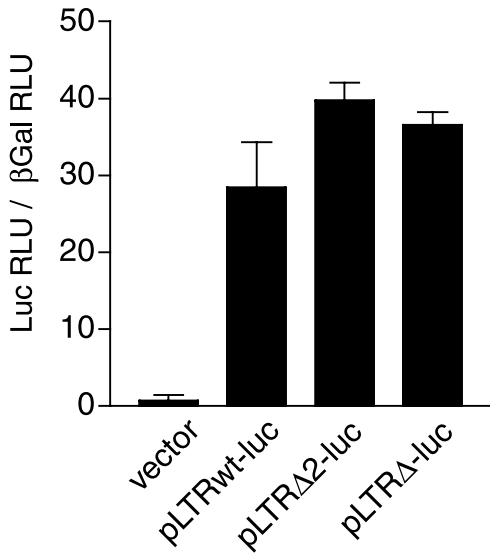


FIG. 7. Transcriptional activity of SIV LTR with U3 deletions. The activity of LTR-luciferase (Luc) constructs in the presence of Tat was measured in electroporated Jurkat E6 cells. To normalize for transfection efficiency, cells were electroporated with both an LTR-luciferase plasmid and a constitutive β-galactosidase (βGal) expression vector. LTR activity was measured as the ratio of luciferase activity to β-galactosidase activity. The mean values obtained for duplicate samples are shown with standard deviations. RLU, relative light units.

SIVmac239Δnef virus, which caused disease in only 1 of 16 rhesus macaques within the same time frame (7). We propose that evolution of viral *nef* sequences contributed to restore the pathogenicity of SIVmac1490, although we cannot rule out that changes in other regions of the genome also played a role in the observed phenotype. Major changes were detected in the SIVmac1490 *nef* gene, notably, the acquisition of an additional deletion, which restored the original *nef* open reading frame in the 3' region. We sought to determine whether these combined deletions in *nef* could contribute to the recovery of a functional

protein. Analysis of Nef properties revealed that the truncated protein Nef-Δ2 retained the capacity to increase viral replication in primary T cells. Other Nef functions such as cell surface receptor downregulation and infectivity enhancement in HeLa cell were lost, suggesting that these properties are not strictly required for SIV pathogenicity. The increase in viral replication conferred by Nef-Δ2 remained lower than that conferred by Nef-WT, which was compatible with the intermediate pathogenicity of the isolate SIVmac1490 compared to that of wild-type SIVmac239 (Fig. 1C and 6C). The parallel observed between in vitro and in vivo phenotypes suggests that Nef-mediated enhancement of viral replication in primary T cells is a key determinant of SIV pathogenicity.

The mechanism responsible for the effect of truncated Nef proteins on viral replication remains to be elucidated. Nef-Δ2 lacks the conserved central regions that form the structural core of the protein and that have been implicated in several Nef properties, including interaction with the SH3 domain of kinases, interaction with PAK kinase, and infectivity enhancement in HeLa cells (reviewed in references 11, 12, 31, and 35). Some of the key residues involved in the interaction of SIV Nef with CD4, MHC-I, and the zeta chain of the CD3 receptor are also missing, which likely accounts for the loss of downregulation of these molecules. Nef-Δ2, however, retains most of the N-terminal and C-terminal flexible regions, which have multiple interaction partners. In particular, the N-terminal fragment contains the bipartite membrane targeting domain that is essential to every Nef function described thus far. The N-terminal region of Nef interacts with a complex formed by Lck and a serine kinase (NAKC) (3) and also binds directly to the p85 subunit of phosphatidylinositol 3-kinase, which can induce antiapoptotic signals (41). Both of these interactions are important for the enhancement of viral replication in T cells and may contribute to the Nef-Δ2 phenotype.

Most residues important for Nef interaction with the cellular trafficking machinery are present in Nef-Δ2, including the N-terminal tyrosine-based motif (Y28xxL,Y39xxS) and the C-

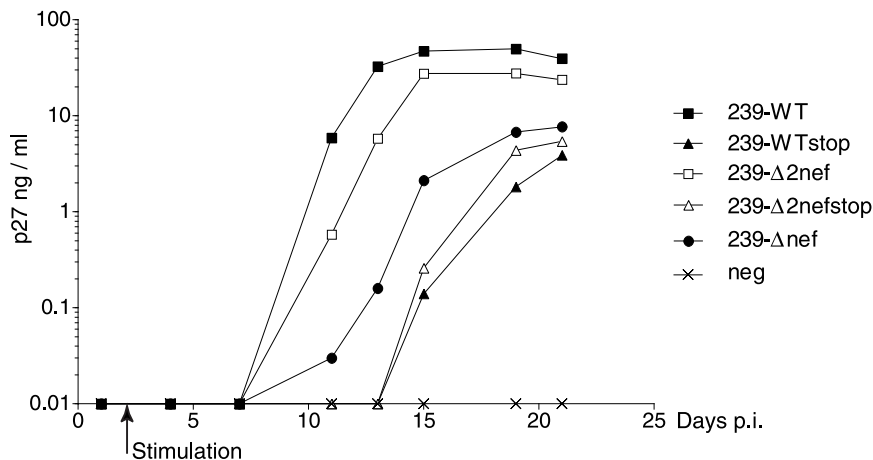


FIG. 8. Introduction of a stop codon in Nef-Δ2 abolishes the enhancement of viral replication in primary cells. Human PBMC were infected with SIV molecular clones that were isogenic except for the presence of a termination codon after the aa 20 of Nef. Compare 239-Δ2nef with 239-Δ2nefstop and 239-WT with 239-WTstop. PBMC were stimulated at day 2 by the addition of PHA and IL-2. Viral replication was monitored for 3 weeks by measuring the amount of SIV Gag p27 antigen in culture supernatants. Results are representative of those from three independent experiments. neg, negative control.

terminal leucine-based motif (L194M), both of which can mediate binding to clathrin adaptor complexes (4). The acidic region that has been implicated in the binding of HIV-1 Nef to PACS, a protein that controls endosome-to-Golgi trafficking, is deleted in Nef- $\Delta 2$ (32), but a putative PACS1 interaction motif is still present in the C-terminal loop region of SIV Nef (12). The conservation of these motifs may account for the vesicular localization of Nef- $\Delta 2$. It should be noted, however, that the distribution of Nef- $\Delta 2$ differed from that of Nef-WT by a more homogeneous repartition in cytoplasmic vesicles. It is possible that the loss of interaction with partners such as CD4 and MHC-I alters the routing of Nef- $\Delta 2$ to vesicular compartments.

The finding that Nef- $\Delta 2$ expression facilitates SIV replication in unstimulated primary T cells but does not increase single-cycle infectivity in HeLa cells indicates that these two properties can be dissociated and are not necessarily attributed to the same function of Nef. In the case of HIV-1 Nef, mutations that impair single-cycle infectivity but not replication in PBMC localize to the N-terminal region (Nef $\Delta 7$ -22) and to the proline motif in the central core region (25, 39). The capacity of HIV-1 Nef to increase viral replication in PBMC has been correlated with its capacity to downregulate CD4 (13, 25). Interestingly, this relationship was not observed for SIV Nef, since the Nef- $\Delta 2$ protein retained the capacity to increase viral replication but failed to downregulate CD4. These observations suggest that similar functions of HIV-1 and SIV Nef can be encoded by different structural determinants, a notion that is also supported by studies of CD4 and MHC-I downregulation (24, 37), and Hck binding (30).

The persistence of sequences coding for Nef- $\Delta 2$ in Rh1490 (7) and their conservation in three out of four inoculated rhesus macaques suggest that these sequences are under positive selection pressure and contribute to the emergence of a virulent phenotype. However, an additional Nef deletion occurred in animal J482, which still progressed to disease. The presence of nonconservative changes in the remaining Nef-coding sequences amplified from this animal (Fig. 2) probably reflects a loss of selection pressure for a functional Nef protein. Therefore, reversion to virulence may also occur through mechanisms that do not primarily depend on Nef. It cannot be ruled out that accumulation of large deletions within the U3 region of the LTR improves HIV and SIV replication in vivo, even though effects on viral transcription appeared to be limited in vitro (this study and references 15 and 33). Improvement of LTR function may account for the progressive accumulation of U3 deletions observed in several LTNP infected with *nef* deletion HIV-1 (10, 21). Large U3 deletions were often accompanied by duplication of NF- κ B and Sp1 binding sites, which may contribute to increasing the efficiency of viral transcription (10). It should be noted that changes in other regions of the genome may also contribute to virulence. For instance, the sequence of SIVmac239 was shown to be less than optimal for viral replication, based on the consistent appearance of the same mutations in *pol* and *rev/env* genes when rhesus macaques were inoculated with virus generated from this molecular clone (1).

There are clear indications that selection for expression of a truncated Nef protein can play a role in reversion to virulence. In the present study, both macaques Rh1490 and L259 experienced a decline in CD4⁺ T cells while infected with a virus

that expressed the truncated 23-kDa protein Nef- $\Delta 2$. In another study, rhesus macaques inoculated with SIVmac239 carrying both a mutated *nef* initiation codon and a 152-bp deletion in *nef* developed AIDS in roughly 50% of cases (34). Reversion to virulence was associated with reopening of the *nef* open reading frame and with the expression of a 25- to 27-kDa Nef protein that was maintained over time. In the case of more limited *nef* deletions, reversion to a virulent phenotype is often accompanied by a repair of missing *nef* sequences. For instance, spontaneous repair of the 12-bp *nef* deletion in clone SIVmacC8 was associated with disease progression in infected rhesus macaques (40). Selection for Nef repair was also evidenced in HIV-1 from one LTNP, for which 36 bp missing in *nef* was partially restored by duplication of adjacent sequences (5). The duplication resulted in the recovery of some Nef functions, including the ability to downregulate MHC-I and to enhance virus infectivity. In the case of point mutations in *nef*, reversion is extremely rapid as demonstrated by the reopening of the *nef* open reading frame in SIVmac239-*nef*stop-infected animals by the second week postinoculation (6, 19). Therefore, selection pressures appear to have different outcomes depending on the nature of the inactivating mutations in *nef*: small deletions and point mutations can be repaired, while larger deletions allow only partial restoration of Nef functions. In the case of the largest deletions, the selective advantage of expressing a truncated Nef protein may be equivalent to or lower than that associated with the loss of U3 sequences, which would account for the accumulation of additional deletions.

The pathogenesis induced by SIV with Nef deletions appeared to differ from that induced by wild-type SIVmac. It was intriguing in particular that animal L257 progressed to disease while maintaining an undetectable viral load. The use of a sensitive real-time PCR assay showed that the concentration of viral RNA in plasma remained below 50 copies/ml even at the time of necropsy. Another animal, L259, had a low viral load at the time of death. We have also observed that, in the long term, certain rhesus macaques inoculated with SIVmac239 Δ *nef* start showing signs of CD4⁺ T-cell decrease, even in the absence of a detectable viral load (unpublished observation). A parallel can be made with findings for some LTNP infected with HIV-1 with *nef* deleted. In the case of a hemophiliac patient infected since 1983, CD4⁺ T-cell counts decreased to 261/mm³ in 1998, even though the plasma viremia remained undetectable throughout the period of observation (14). In the Sydney Blood Bank cohort, three patients who showed signs of progression had a detectable viral load, although the number of viral RNA copies in plasma remained moderate (median of fewer than 2,850 copies/ml) with respect to the slope of CD4⁺ T-cell depletion (23). These observations suggest that pathogenic progression induced by HIV and SIV with *nef* deleted differs from that induced by the wild-type virus, either in the extent of viral replication or in the efficiency of trapping of viral particles in lymphoid organs. Further analysis of specific pathogenic traits associated with lentiviruses with *nef* deleted should provide new insights into the links between viral replication, CD4⁺ T-cell depletion, and immune system dysfunction.

ACKNOWLEDGMENTS

We thank Agegnehu Gettie for help with animal experiments; Paul Luciw for the anti-SIV Nef serum; Zhiwei Chen, Pierre Charneau,

Nathaniel Landau, and Rong Liu for cell lines; and Toshiaki Kodama, Ronald Desrosiers, and Paul Bieniasz for plasmids. We are grateful to Amanda Brown for helpful discussions. Plasmid p239SpE3'ΔNef (reagent no. 2477) was obtained from Ronald Desrosiers through the AIDS Research and Reference Reagent Program, Division of AIDS, NIAID, NIH.

This study was supported by NIH grant AI38532, Tulane Regional Primate Research Center base grant RR00164, the Aaron Diamond Foundation, and the Pasteur Institute.

REFERENCES

- Alexander, L., L. Denekamp, S. Czajak, and R. C. Desrosiers. 2001. Suboptimal nucleotides in the infectious, pathogenic simian immunodeficiency virus clone SIVmac239. *J. Virol.* **75**:4019–4022.
- Baba, T. W., V. Liska, A. H. Khimani, N. B. Ray, P. J. Dailey, D. Penninck, R. Bronson, M. F. Greene, H. M. McClure, L. N. Martin, and R. M. Ruprecht. 1999. Live attenuated, multiply deleted simian immunodeficiency virus causes AIDS in infant and adult macaques. *Nat. Med.* **5**:194–203.
- Baur, A. S., G. Sass, B. Laffert, D. Willbold, C. Cheng-Mayer, and B. M. Peterlin. 1997. The N-terminus of Nef from HIV-1/SIV associates with a protein complex containing Lck and a serine kinase. *Immunity* **6**:283–291.
- Bresnahan, P. A., W. Yonemoto, and W. C. Greene. 1999. Cutting edge: SIV Nef protein utilizes both leucine- and tyrosine-based protein sorting pathways for down-regulation of CD4. *J. Immunol.* **163**:2977–2981.
- Carl, S., R. Daniels, A. J. Iafate, P. Easterbrook, T. C. Greenough, J. Skowronski, and F. Kirchhoff. 2000. Partial “repair” of defective NEF genes in a long-term nonprogressor with human immunodeficiency virus type 1 infection. *J. Infect. Dis.* **181**:132–140.
- Chakrabarti, L., V. Baptiste, E. Khatissian, M. C. Cumont, A. M. Aubertin, L. Montagnier, and B. Hurler. 1995. Limited viral spread and rapid immune response in lymph nodes of macaques inoculated with attenuated simian immunodeficiency virus. *Virology* **213**:535–548.
- Connor, R. I., D. C. Montefiori, J. M. Binley, J. P. Moore, S. Bonhoeffer, A. Gettie, E. A. Fenamore, K. E. Sheridan, D. D. Ho, P. J. Dailey, and P. A. Marx. 1998. Temporal analyses of virus replication, immune responses, and efficacy in rhesus macaques immunized with a live, attenuated simian immunodeficiency virus vaccine. *J. Virol.* **72**:7501–7509.
- Dailey, P. J., M. Zamroud, R. Kelso, J. Kolberg, and M. Urdea. 1995. Quantitation of simian immunodeficiency virus (SIV) RNA in plasma of acute and chronically infected macaques using a branched DNA (bDNA) signal amplification assay. *J. Med. Primatol.* **95**:209.
- Daniel, M. D., F. Kirchhoff, S. C. Czajak, P. K. Sehgal, and R. C. Desrosiers. 1992. Protective effect of a live attenuated SIV vaccine with a deletion in the *nef* gene. *Science* **258**:19381.941.
- Deacon, N. J., A. Tsykin, A. Solomon, K. Smith, M. Ludford-Menting, D. J. Hooker, D. A. McPhee, A. L. Greenway, A. Ellett, C. Chatfield, et al. 1995. Genomic structure of an attenuated quasi species of HIV-1 from a blood transfusion donor and recipients. *Science* **270**:988–991.
- Fackler, O. T., and A. S. Baur. 2002. Live and let die. Nef functions beyond HIV replication. *Immunity* **16**:493–497.
- Geyer, M., O. T. Fackler, and B. M. Peterlin. 2001. Structure-function relationships in HIV-1 Nef. *EMBO Rep.* **2**:580–585.
- Glushakova, S., J. Munch, S. Carl, T. C. Greenough, J. L. Sullivan, L. Margolis, and F. Kirchhoff. 2001. CD4 down-modulation by human immunodeficiency virus type 1 Nef correlates with the efficiency of viral replication and with CD4⁺ T-cell depletion in human lymphoid tissue ex vivo. *J. Virol.* **75**:10113–10117.
- Greenough, T. C., J. L. Sullivan, and R. C. Desrosiers. 1999. Declining CD4 T-cell counts in a person infected with nef-deleted HIV-1. *N. Engl. J. Med.* **340**:236–237.
- Ilyinskii, P. O., M. D. Daniel, M. A. Simon, A. A. Lackner, and R. C. Desrosiers. 1994. The role of upstream U3 sequences in the pathogenesis of simian immunodeficiency virus-induced AIDS in rhesus monkeys. *J. Virol.* **68**:5933–5944.
- Ilyinskii, P. O., and R. C. Desrosiers. 1996. Efficient transcription and replication of simian immunodeficiency virus in the absence of NF-κB and Sp1 binding elements. *J. Virol.* **70**:3118–3126.
- Ilyinskii, P. O., M. A. Simon, S. C. Czajak, A. A. Lackner, and R. C. Desrosiers. 1997. Induction of AIDS by simian immunodeficiency virus lacking NF-κB and SP1 binding elements. *J. Virol.* **71**:1880–1887.
- Johnson, R. P., and R. C. Desrosiers. 1998. Protective immunity induced by live attenuated simian immunodeficiency virus. *Curr. Opin. Immunol.* **10**:436–443.
- Kestler, H. W., III, D. J. Ringler, K. Mori, D. Panicalli, P. Sehgal, M. D. Daniel, and R. C. Desrosiers. 1991. Importance of the nef gene for maintenance of high virus loads and for development of AIDS. *Cell* **65**:651–662.
- Kirchhoff, F., P. J. Easterbrook, N. Douglas, M. Troop, T. C. Greenough, J. Weber, S. Carl, J. L. Sullivan, and R. S. Daniels. 1999. Sequence variations in human immunodeficiency virus type 1 Nef are associated with different stages of disease. *J. Virol.* **73**:5497–5508.
- Kirchhoff, F., T. C. Greenough, D. B. Brettler, J. L. Sullivan, and R. C. Desrosiers. 1995. Absence of intact nef sequences in a long-term survivor with nonprogressive HIV-1 infection. *N. Engl. J. Med.* **332**:228–232.
- Kirchhoff, F., H. W. Kestler III, and R. C. Desrosiers. 1994. Upstream U3 sequences in simian immunodeficiency virus are selectively deleted in vivo in the absence of an intact *nef* gene. *J. Virol.* **68**:2031–2037.
- Learmont, J. C., A. F. Geczy, J. Mills, L. J. Ashton, C. H. Raynes-Greenow, R. J. Garsia, W. B. Dyer, L. McIntyre, R. B. Oelrichs, D. I. Rhodes, N. J. Deacon, and J. S. Sullivan. 1999. Immunologic and virologic status after 14 to 18 years of infection with an attenuated strain of HIV-1. A report from the Sydney Blood Bank Cohort. *N. Engl. J. Med.* **340**:1715–1722.
- Lock, M., M. E. Greenberg, A. J. Iafate, T. Swigut, J. Muench, F. Kirchhoff, N. Shohdy, and J. Skowronski. 1999. Two elements target SIV Nef to the AP-2 clathrin adaptor complex, but only one is required for the induction of CD4 endocytosis. *EMBO J.* **18**:2722–2733.
- Lundquist, C. A., M. Tobiume, J. Zhou, D. Unutmaz, and C. Aiken. 2002. Nef-mediated downregulation of CD4 enhances human immunodeficiency virus type 1 replication in primary T lymphocytes. *J. Virol.* **76**:4625–4633.
- Malenbaum, S. E., D. Yang, L. Cavacini, M. Posner, J. Robinson, and C. Cheng-Mayer. 2000. The N-terminal V3 loop glycan modulates the interaction of clade A and B human immunodeficiency virus type 1 envelopes with CD4 and chemokine receptors. *J. Virol.* **74**:11008–110016.
- Martin-Serrano, J., K. Li, and P. D. Bieniasz. 2002. Cyclin T1 expression is mediated by a complex and constitutively active promoter and does not limit human immunodeficiency virus type 1 Tat function in unstimulated primary lymphocytes. *J. Virol.* **76**:208–219.
- Metzner, K. J., X. Jin, F. V. Lee, A. Gettie, D. E. Bauer, M. Di Mascio, A. S. Perelson, P. A. Marx, D. D. Ho, L. G. Kostrikis, and R. I. Connor. 2000. Effects of in vivo CD8(+) T cell depletion on virus replication in rhesus macaques immunized with a live, attenuated simian immunodeficiency virus vaccine. *J. Exp. Med.* **191**:1921–1931.
- Miller, M. D., M. T. Warmerdam, I. Gaston, W. C. Greene, and M. B. Feinberg. 1994. The human immunodeficiency virus *nef* gene product: a positive factor for viral infection and replication in primary lymphocytes and macrophages. *J. Exp. Med.* **179**:101–113.
- Picard, C., A. Greenway, G. Holloway, D. Olive, and Y. Collette. 2002. Interaction with simian hck tyrosine kinase reveals convergent evolution of the nef protein from simian and human immunodeficiency viruses despite differential molecular surface usage. *Virology* **295**:320–327.
- Piguet, V., O. Schwartz, S. Le Gall, and D. Trono. 1999. The downregulation of CD4 and MHC-I by primate lentiviruses: a paradigm for the modulation of cell surface receptors. *Immunol. Rev.* **168**:51–63.
- Piguet, V., L. Wan, C. Borel, A. Mangasarian, N. Demareux, G. Thomas, and D. Trono. 2000. HIV-1 Nef protein binds to the cellular protein PACS-1 to downregulate class I major histocompatibility complexes. *Nat. Cell Biol.* **2**:163–167.
- Pohlmann, S., S. Floss, P. O. Ilyinskii, T. Stamminger, and F. Kirchhoff. 1998. Sequences just upstream of the simian immunodeficiency virus core enhancer allow efficient replication in the absence of NF-κB and Sp1 binding elements. *J. Virol.* **72**:5589–5598.
- Sawai, E. T., M. S. Hamza, M. Ye, K. E. Shaw, and P. A. Luciw. 2000. Pathogenic conversion of live attenuated simian immunodeficiency virus vaccines is associated with expression of truncated Nef. *J. Virol.* **74**:2038–2045.
- Sawai, E. T., I. H. Khan, P. M. Montbriand, B. M. Peterlin, C. Cheng-Mayer, and P. A. Luciw. 1996. Activation of PAK by HIV and SIV Nef: importance for AIDS in rhesus macaques. *Curr. Biol.* **6**:1519–1527.
- Spina, C. A., T. J. Kwol, M. Y. Chowes, J. C. Guatelli, and D. D. Richman. 1994. The importance of nef in the induction of human immunodeficiency virus type 1 replication from primary quiescent CD4 lymphocytes. *J. Exp. Med.* **179**:115–123.
- Swigut, T., A. J. Iafate, J. Muench, F. Kirchhoff, and J. Skowronski. 2000. Simian and human immunodeficiency virus Nef proteins use different surfaces to downregulate class I major histocompatibility complex antigen expression. *J. Virol.* **74**:5691–5701.
- Switzer, W. M., S. Wiktor, V. Soriano, A. Silva-Graca, K. Mansinho, I. M. Coulbaly, E. Ekpini, A. E. Greenberg, T. M. Folks, and W. Heneine. 1998. Evidence of Nef truncation in human immunodeficiency virus type 2 infection. *J. Infect. Dis.* **177**:65–71.
- Welker, R., M. Harris, B. Cardel, and H. G. Krausslich. 1998. Virion incorporation of human immunodeficiency virus type 1 Nef is mediated by a bipartite membrane-targeting signal: analysis of its role in enhancement of viral infectivity. *J. Virol.* **72**:8833–8840.
- Whatmore, A. M., N. Cook, G. A. Hall, S. Sharpe, E. W. Rud, and M. P. Cranage. 1995. Repair and evolution of Nef in vivo modulates simian immunodeficiency virus virulence. *J. Virol.* **69**:5117–5123.
- Wolf, D., V. Witte, B. Laffert, K. Blume, E. Stromer, S. Trapp, P. d'Aloja, A. Schurmann, and A. S. Baur. 2001. HIV-1 Nef associated PAK and PI3-kinases stimulate Akt-independent Bad-phosphorylation to induce anti-apoptotic signals. *Nat. Med.* **7**:1217–1224.
- Wyand, M. S., K. Manson, D. C. Montefiori, J. D. Lifson, R. P. Johnson, and R. C. Desrosiers. 1999. Protection by live, attenuated simian immunodeficiency virus against heterologous challenge. *J. Virol.* **73**:8356–8363.